

Disruption Mitigation with Plasma Jets for ITER

I. N. Bogatu 1), J. R. Thompson 1), S. A. Galkin 1), J. S. Kim 1), and HyperV Technologies Corp. Team 2)

1) FAR-TECH, Inc., San Diego, California 92121, USA

2) HyperV Technologies Corp., Chantilly, Virginia 20151, USA

E-mail contact of main author: nbogatu@far-tech.com

Abstract. Disruption mitigation in ITER requires a reliable technique with real-time capability. Impurity injection has been proposed to convert the plasma energy density (~ 1 GJ in 840 m^3) into radiation power in ~ 1 ms and to increase the electron density by two orders of magnitude throughout the plasma cross section so as to achieve suppression of runaway electrons avalanche. However, once the impurity atoms are ionized in the thin outer layer of the tokamak plasma, they can no longer penetrate the confining magnetic field unless they have high velocity. Based on experimental and modeling results with injection of gas, pellets, and liquids, it appears very difficult to achieve simultaneously, deep penetration into the core plasma, efficient ablation, impurity assimilation, and an increase of electron density on the required time scale. FAR-TECH proposed the innovative idea of producing and using hyper-velocity (>30 km/s), high-density ($>10^{17} \text{ cm}^{-3}$) plasma jets of C_{60} -fullerene. The high ram pressure of the C_{60}/C plasma jets allows them to penetrate the tokamak hot plasma, overcoming the confining magnetic field pressure, and delivering the needed impurity mass required in less than 1 ms. For this purpose a large mass of explosively sublimated C_{60} molecular gas, generated by a solid state pulsed power driven source containing both TiH_2 grains and C_{60} powder, is ionized and accelerated as a plasma slug in a coaxial plasma accelerator. Our 3D simulations using the LSP PIC code show that a heavy C_{60} plasmoid penetrates deeply, as a compact structure, through a transverse magnetic barrier, demonstrating self-polarization and magnetic field expulsion effects. A prototype of a coaxial plasma gun with a $\text{TiH}_2/\text{C}_{60}$ source injector cartridge is under development for a small scale, proof-of-principle experiment which could be demonstrated a tokamak such as DIII-D. We report here on the experimental characterization of the prototype solid state, pulsed power driven $\text{TiH}_2/\text{C}_{60}$ injector cartridge.

1. Introduction

A disruption mitigation scheme must convert ITER plasma energy density (~ 1 GJ/ 840 m^3) into radiation within 1 ms and suppress runaway electrons avalanche by an increase of the electron density to the Rosenbluth density throughout the plasma cross section [1] (~ 100 times increase due to free and bound electrons from partially ionized impurity atoms). The principle solution is considered to be impurity injection into the confined plasma.

A number of alternate approaches to impurity injection have been investigated by others, including massive (neutral) gas injection in the scrape-off layer region [2, 3, 4] and the injection of much higher density pellets or liquids which can achieve penetration, but have to rely on efficient ablation and impurity assimilation by stopping it in the cold plasma of the current quench phase within the required time scale [5]. Experiments have demonstrated the difficulty to project the results to ITER [6].

Fueling experiments on the small Globus-M tokamak [7, 8, 9, 10, 11] demonstrated deep (to half minor radius) and fast penetration into a tokamak plasma and its confining magnetic field, of a high-velocity (~ 140 km/sec), dense ($\sim 2 \times 10^{16} \text{ cm}^{-3}$) plasma jet with a mass of $17 \mu\text{g}$, accelerated using a coaxial plasma gun. The electron density was shown to increase (double) much faster (<0.5 ms) than for fast gas jet injection (~ 2.5 ms) and to be better distributed throughout plasma cross section.

FAR-TECH proposed and is pursuing the innovative idea of producing and using high-velocity (>30 km/s), high-density ($>10^{17}$ cm $^{-3}$) plasma jets of C $_{60}$ -fullerene [12]. The high velocity leads to a sufficient ram pressure of the plasma jets to allow penetration into the tokamak hot plasma, overcoming the confining magnetic field pressure, and delivering the mass required in less than 1 ms. For disruption mitigation a large mass of explosively sublimated C $_{60}$ molecular gas, generated by a solid state, pulsed power driven source containing both TiH $_2$ grains and C $_{60}$ micron size powder, is ionized and accelerated as a plasma slug in a coaxial plasma accelerator as detailed in [13] and presented in FIG. 1.

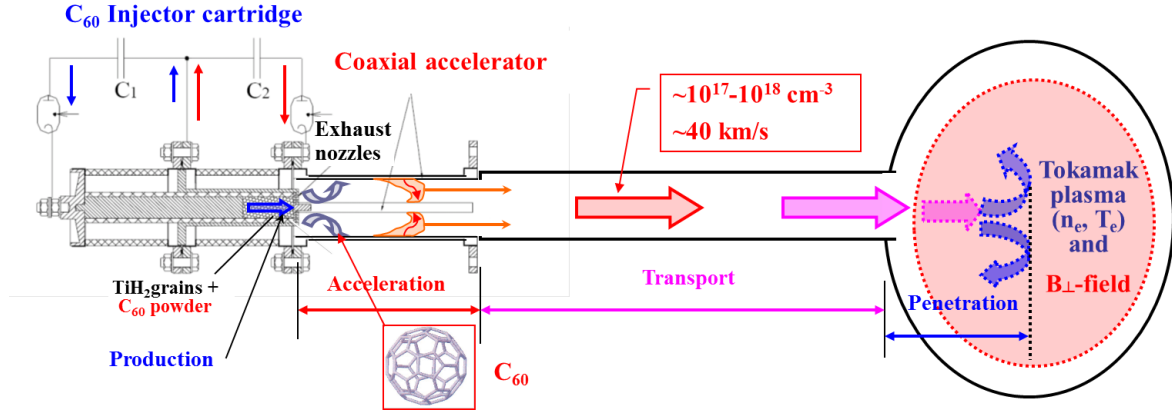


FIG. 1. Disruption mitigation scheme with a C $_{60}$ plasma jet from a coaxial plasma gun.

Modeling of a pulsed power heated cylindrical resistor composed of many packed small TiH $_2$ spherical grains and micron sized C $_{60}$ powder suggested that hot H $_2$ gas generation, followed by C $_{60}$ powder sublimation by the hot hydrogen, can take place within $\sim 10-20$ μ s [13]. Simulations with an extended physics plasma slug model, benchmarked against Globus-M coaxial gun data, shows that a 100 kJ capacitive driver should be capable of accelerating a mass of 30 mg to a high velocity of 30-40 km/s within a coaxial gun length of about 50 cm, realistic parameters for a small scale proof-of-principle demonstration.

LSP PIC code 3D [14] simulations of plasmoid ($n=2 \times 10^{16}$ cm $^{-3}$, $T=1$ eV, $v_0=30$ km/s), penetration through a transverse vacuum magnetic barrier ($B=0.1$ T, in the range of the Globus-M tokamak) (see FIG. 2) show that a heavy molecular C $_{60}^+$ plasmoid of 288 μ g penetrates deeply as a compact structure, exhibiting self-polarization and magnetic field expulsion effects, while a C $^+$ plasmoid of 4.8 μ g is stopped. Further simulations with C $_{60}^+$ and C $^+$ plasmoids of the same mass showed that C $_{60}^+$ deep penetration takes place even if its density is 60 times lower.

A prototype of coaxial plasma gun with a pulsed power based TiH $_2$ /C $_{60}$ source injector cartridge is under development for a small scale, proof-of-principle experiment ($m=30$ mg C $_{60}$ /C, $v \sim 30$ km/s, $E_{\text{Driver}}=100$ kJ) which could be demonstrated on a tokamak such as DIII-D. This paper presents the results from initial characterization of the pulsed power based TiH $_2$ /C $_{60}$ source injector cartridge.

2. Experimental Setup - TiH $_2$ /C $_{60}$ Injector Cartridge

The pulsed power based TiH $_2$ /C $_{60}$ injector cartridge is shown in FIG. 3, indicating its major sub-components. The core of the injector is the reservoir of TiH $_2$ grains and C $_{60}$ powder, held under mechanical compression up against the exhaust nozzles by a spring loaded electrode plunger. Power is delivered to the injector via coaxial cables from a capacitive driver.

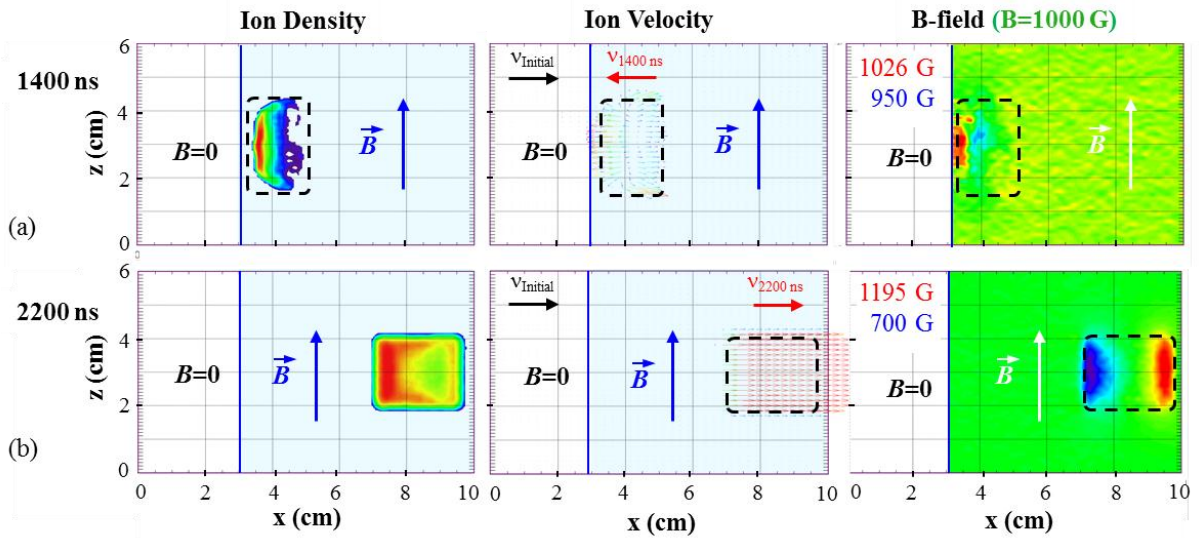


FIG. 2. LSP code results of plasmoid penetration through transverse magnetic barrier: a) C^+ shows field expulsion and is stopped; b) C_{60}^+ penetrates by self-polarization deeper as a compact structure.

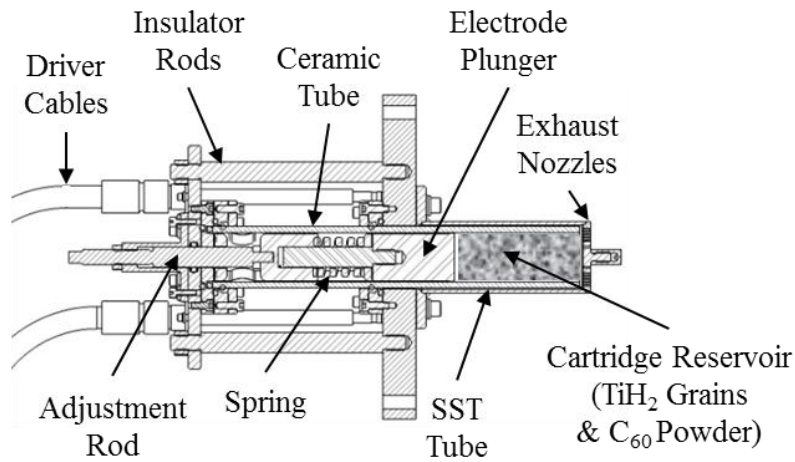


FIG. 3. Pulsed power based TiH_2/C_{60} injector cartridge.

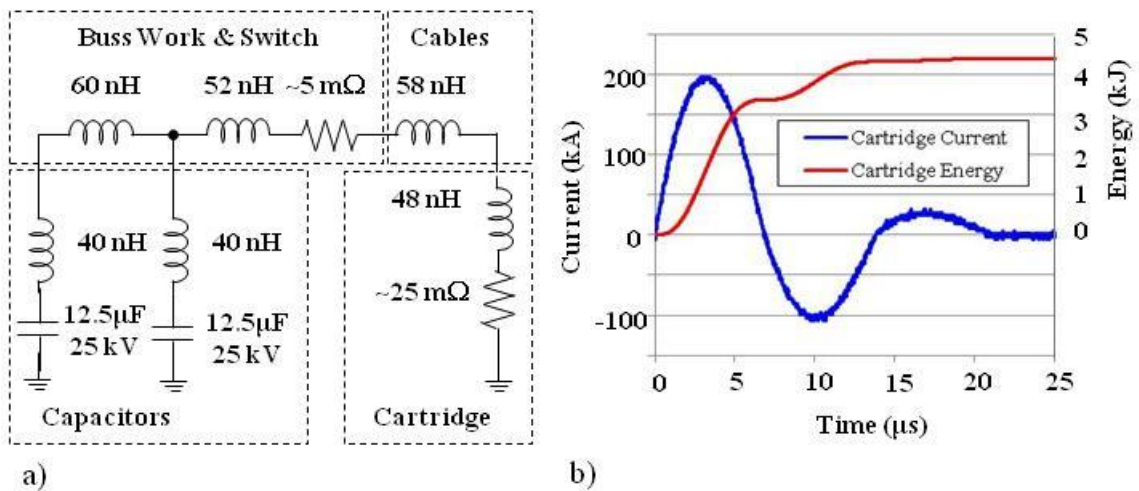


FIG. 4. a) Equivalent circuit for cartridge capacitive driver and injector cartridge, b) typical injector cartridge drive current waveform and energy deposition time history.

The equivalent circuit for the $\text{TiH}_2/\text{C}_{60}$ injector cartridge's capacitive driver is shown in FIG. 4a, utilizing two capacitors capable of storing up to 7.5 kJ when charged to 25 kV (initial testing began with only one capacitor). FIG. 4b shows the injector cartridge drive current waveform and the energy deposition time history for a typical 20 kV shot. During the current pulse, the cartridge resistance rises rapidly from an initial resistance of $\sim 5 \text{ m}\Omega$, in the case of this shot to 18 $\text{m}\Omega$ by the first current peak, and reaching 32 $\text{m}\Omega$ at the second current peak, reflecting a change in grain/powder temperature. The driver to cartridge energy coupling efficiency is estimated at $\sim 80\%$.

3. Injector Cartridge Source Results

Two experimental test series were performed. The first to test the capability of the injector cartridge to provide the mass of H_2 necessary to sublime the C_{60} , utilizing TiH_2 grains only. The second to characterize the C_{60} output of a combined TiH_2 grains and C_{60} powder injector cartridge fill.

The injector cartridge shown in FIG. 3 was mounted on a vacuum chamber at the HyperV Technologies Corp. facility. The capacitive driver, shown in FIG. 5a, with an option of using one or both capacitors, provided cartridge currents up to 264 kA, resulting in the deposition of up to $\sim 5 \text{ kJ}$ in the injector cartridge, in a time scale of $\sim 20\text{-}35 \mu\text{s}$.

The diagnostics used to characterize the ejected molecular gas jet were the following: ballistic pendulum for momentum [15], laser interferometer for density [15], piezoelectric pressure probe for stagnation pressure (used only in second test series) [16], and vacuum gauge for the post-shot pressure, allowing an estimate of the total H_2 mass ejected.

3.1. TiH_2 Grains only

The cartridge reservoir shown in FIG. 3, filled with $\geq 1 \text{ mm}$ TiH_2 grains, had a diameter of 31.8 mm and length of 80 mm. The total mass of TiH_2 grains was $\sim 120 \text{ g}$, with a packing density of $\sim 66\%$. The DC resistance was observed to decrease with grain compression from $\sim 2 \Omega$ uncompressed, to $\sim 120 \text{ m}\Omega$ with a compression force of $\sim 820 \text{ N}$, primarily because of an increase in the number of grain contact points and their associated areas, caused by crushing. The grains are transiently heated mainly at their contact areas where the current density reaches very high values leading to melting and fusing of TiH_2 at their contact points. Moreover, because of the transient nature of the pulsed power drive, the effective current skin depth, which is estimated to be $< 500 \mu\text{m}$, results in an increase of the effective electrical resistivity over that of a static resistance measurement, and as a consequence, a reduction of the initially heated TiH_2 mass. These two effects lead to more efficient heating, and hence higher local temperatures at the TiH_2 grain surfaces. Thermal heat conduction plays a minimal role in the time scales associated with cartridge operation.

The transient evolution of the ejected H_2 jet density was determined from chordal line-integrated laser interferometry located $\sim 10 \text{ mm}$ downstream of the exhaust nozzles. The data in FIG. 5a show that the jet average density increases with driver energy up to $\sim 3 \times 10^{18} \text{ cm}^{-3}$ in $\sim 50 \mu\text{s}$, for the 7.2 kJ shot. The observed delay in density rise relative to the cartridge current drive gives an estimated velocity for the initial H_2 of $\sim 1 \text{ km/s}$.

The total momentum of the gas jet was determined from the motion of a ballistic pendulum. The maximum amplitude (swing) was recorded using a time-integrated optical image of the pendulum motion, as indicated by a light trace created by a LED light source mounted on the pendulum disk. The amplitude of the pendulum motion, hence the delivered momentum transfer from the ejected H₂ gas, was observed to increase with driver energy. Using the interferometry inferred initial H₂ velocity of 1 km/s, the total exhausted H₂ mass was estimated as ~2 mg for the 7.2 kJ driver shot.

The post-shot pressure in the vacuum chamber provided an additional measure of the total mass of ejected H₂ gas. As shown in FIG. 5b, the driver energy dependence of the H₂ mass determined from post-shot pressure followed those of the pendulum inferred mass. The differences between the two estimates are a measure of the uncertainties in the final gas temperature, taken as room temperature, and the mass weighted mean H₂ gas velocity, expected to be less than 1 km/s.

We are currently performing 2D fully compressible gas dynamics simulations using FAR-TECH's computational fluid dynamics code GJET-2D [17], for the gas ejection through the nozzles and plan to use the results to guide the optimization of the cartridge nozzle profile design. FIG. 6 shows an example of the simulation results for H₂ compared with the interferometry, for a simple cartridge model where the equivalent area of the 264 small nozzles is approximated with a single nozzle with circular cross section of 6.73 mm radius. The initial parameters used in the example were as follows: density in the cartridge $n=3\times 10^{19}$ cm⁻³, gas temperature $T_g=700$ K, gas atomic mass units $A=2$ (for H₂), adiabatic coefficient $\gamma=1.35$ (for hot H₂). Simulation with this simple nozzle model can reproduce the characteristic shape of the downstream chordal line-integrated downstream densities obtained from experiment (the relative vertical scaling for the two data sets is arbitrary). Work is currently underway to refine the cartridge model to have multiple gas nozzles (annular shells in r-z model geometry), more realistically simulating the physical configuration. An absolute comparison of magnitude will then be made with the improved cartridge model.

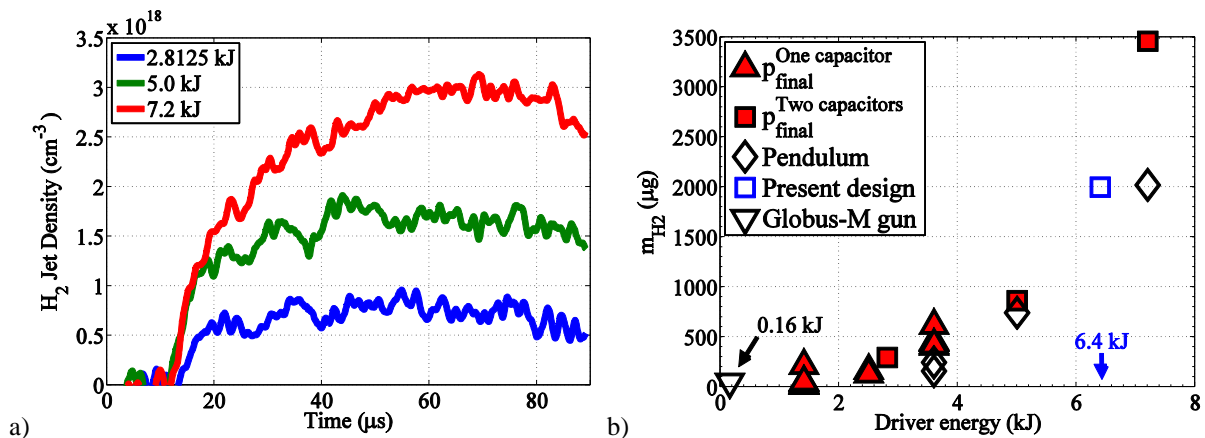


FIG. 5. a) H₂ jet density time dependence for three values of driver energy, b) H₂ mass as a function of driver energy as determined from post-shot vacuum pressure and ballistic pendulum motion.

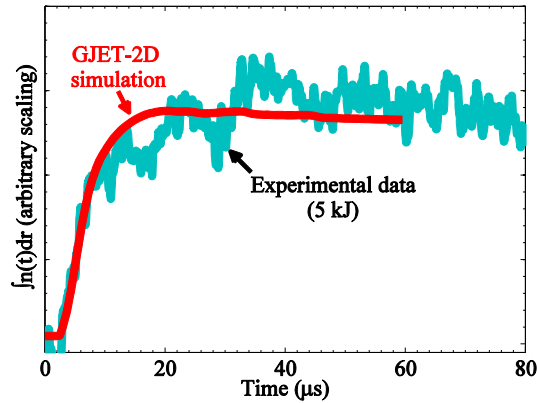


FIG. 6. GJET-2D code results for simple cartridge model compared to interferometry data.

3.2. TiH₂ Grains and C₆₀ Powder

As our aim is to produce the large mass of C₆₀ (at least 30 mg) for our proof-of-principle experiment on a tokamak such as DIII-D, we coated and mixed the TiH₂ grains [13] with a fine C₆₀ powder [18]. As C₆₀ is a semiconductor, the resistivity of the cartridge was found to increase, leading to an enhanced driver to cartridge energy coupling efficiency. We performed all tests with the TiH₂/C₆₀ cartridge using 5 kJ of stored driver energy. The diagnostics used were the same as for the cartridge with TiH₂ grains only, with the addition of a pressure probe.

The pressure probe provided a measurement of the stagnation pressure, $\rho v^2/2$. The pressure probe was located ~ 10 mm downstream of the exhaust nozzles. Because of the electrical noise environment, the valid signal begins at the end of the current pulse as shown in FIG. 7. The gas jet in this series is expected to be composed of H₂ and C₆₀, where the C₆₀ density is expected to be ~ 10 times lower than that of H₂, because it is estimated that it takes about ten H₂ hot molecules to sublimate one C₆₀ molecule. The first pressure peak has a characteristic time profile similar of that observed in the interferometry with TiH₂ only, and is expected to be dominated by H₂ (unfortunate there was no pressure probe data for the TiH₂ series). The second pressure peak is expected to be dominated by the 3-5 times lower velocity C₆₀. The observed first stagnation peak pressure of ~ 36 kPa leads to an evaluated H₂ density of $\sim 2 \times 10^{19}$ cm⁻³ when using the velocity of ~ 1 km/s based on the TiH₂ grains only test results. The observed second stagnation peak pressure of ~ 20 kPa leads to an estimated C₆₀ density of $\sim 8 \times 10^{17}$ cm⁻³, using one-fifth the H₂ velocity, 0.2 km/s.

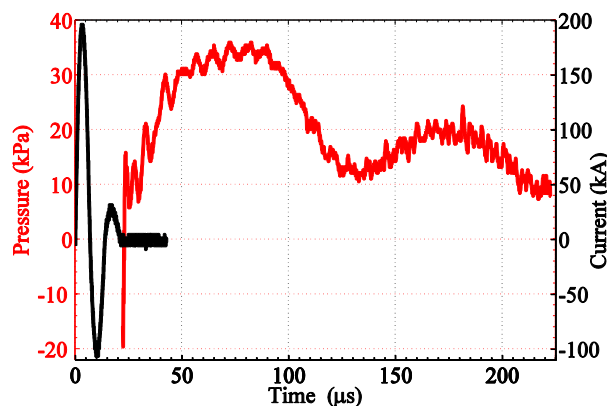


FIG. 7. Downstream pressure probe signal overlaid with the TiH₂/C₆₀ cartridge current.

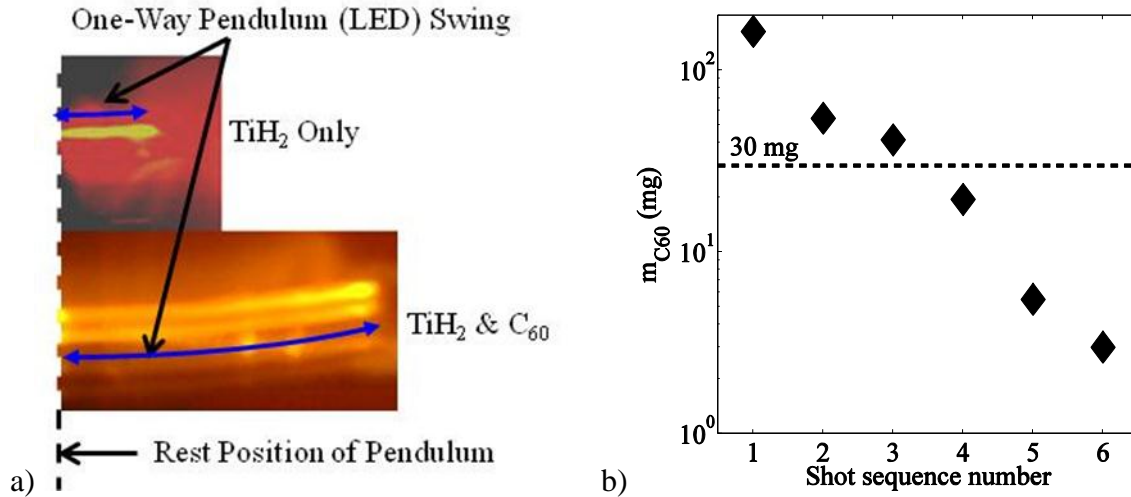


FIG. 8. a) Pendulum amplitude data: TiH₂ only (top) and TiH₂/C₆₀ (bottom); b) ejected C₆₀ mass as a function of shot sequence number from the pendulum data based on a C₆₀ jet component velocity of 0.2 km/s.

FIG. 8a displays time-integrated optical images, showing the magnitude of the pendulum amplitude for two shots taken with the same 5 kJ driver energy, however, with different cartridge loadings. The upper image is for a shot with TiH₂ only, while the lower image is for a combined TiH₂ and C₆₀ loading. The pendulum swing amplitude for the combined TiH₂ and C₆₀ is clearly much larger than for the TiH₂ only, resulting into a momentum transfer ~32 times larger. The very large mass ratio of 360, between C₆₀ and H₂, cannot be compensated by the C₆₀:H₂ velocity ratio of ~0.2 and density ratio of ~0.1, thus the momentum transfer is dominated by the C₆₀ jet component. The estimated C₆₀ jet mass based on the pendulum swing amplitude is presented for several shots in FIG. 8b, plotted as a function of the shot sequence number for the same cartridge fill. The values assume C₆₀ dominance and an average velocity of 0.2 km/s.

4.0 Summary and Future Work

A pulsed power based, high density, fast C₆₀ source has been demonstrated. C₆₀ mass ejection in excess of 30 mg, on a few hundred microsecond time scale has been achieved. This mass level meets our requirements for the source component of a sub-millisecond disruption mitigation system appropriate for a proof-of-principle demonstration.

Continuing work includes the design and fabrication of the coaxial accelerator component of the disruption mitigation system. Coupled to the C₆₀ source, this component will accelerate the C₆₀ mass to a velocity of ~30 km/s, thereby imparting an appropriate ram pressure relative to magnetic field pressure for the penetration of the C₆₀ mass into the tokamak plasma. Once assembled, work will focus on the demonstration of the full prototype disruption mitigation system, with the injection of the high velocity C₆₀ mass through a magnetic field characteristic of that found in DIII-D.

The authors would like to acknowledge F. D. Witherspoon, A. Case, S. Brockington, R. Bomgardner, and S. Messer of HyperV Technologies Corp. for providing the test facility and diagnostic support, as well as, for many fruitful discussions.

Work supported by the US-DOE under DE-FG02-08ER85196 SBIR grant.

References

- [1] ROSENBLUTH, M. N., et al., "Runaway electrons and fast plasma shutdown", Fusion Energy (Proc. 16th Intl. Conf. Montreal, 1996) IAEA, Vienna, vol 2, p. 979 (1997).
- [2] WHYTE, D. G., et al., "Mitigation of Tokamak Disruptions Using High-Pressure Gas Injection", Phys. Rev. Lett. **89** (2002) 055001.
- [3] HOLLMANN, E. et al., "Measurement of Impurity and Heat Dynamics During Noble Gas Jet-Initiated Fast Plasma Shutdown for Disruption Mitigation in DIII-D", Fusion Energy (Proc. 20th Conf. Vilamoura, 2004) IAEA, Vienna, CD-ROM file EX/10-6R.
- [4] GRANETZ, R., et al., "Gas Jet Disruption Mitigation Studies on Alcator C-Mod and DIII-D", 21st IAEA Fusion Energy Conference Chengdu, China, October 16-22, 2006, CD-ROM file EX/4-3.
- [5] WHYTE, D. G., et al., "Studies of Requirements for ITER Disruption Mitigation Systems", 22nd IAEA Fusion Energy Conference 13-18 October 2008 Geneva, Switzerland, CD-ROM file IT/P6-18.
- [6] STAMBAUGH, R., "Review of ITER Physics Issues and Possible Approaches to Their Solution", 21st IAEA Fusion Energy Conference Chengdu, China, October 16-22, 2006.
- [7] VORONIN, A.V., et al., "High kinetic energy plasma jet generation and its injection into the Globus-M spherical tokamak", Nucl. Fusion **45** (2005) 1039.
- [8] VORONIN, A. V., et al., "Progress of the Intense Jet Fuelling Source", 33rd EPS Conference on Plasma Phys. Rome, 19 - 23 June 2006 ECA Vol.**30I**, P-4.105 (2006).
- [9] VORONIN, A.V., et al., "High Kinetic Energy Jet Injection into Globus-M Spherical Tokamak", IAEA 2006 Topic: EX/P3-18.
- [10] GUSEV, V. K., et al., "Overview of Globus-M Spherical Tokamak Results", 11th IST Workshop, Chengdu, China, October 11-23, 2006.
- [11] GUSEV, V. K., et al., "Density limits and control in the Globus-M spherical tokamak", Nucl. Fusion **46**, S584 (2006).
- [12] BOGATU, I. N., et al., "Hyper-Velocity Fullerene-Dusty Plasma Jets for Disruption Mitigation", J. Fusion Energy, **27**, 6 (2008).
- [13] BOGATU, I. N., et al., "C₆₀-Fullerene Hyper-Velocity High-Density Plasma Jets for MIF and Disruption Mitigation", J. Fusion Energy **28**, 144 (2009).
- [14] WELCH, D. R., et al., "Simulation techniques for heavy ion fusion chamber transport", Nucl. Inst. Meth. Phys. Res. A **464**, 134 (2001).
- [15] WITHERSPOON, F. D., et al., "A contoured gap coaxial plasma gun with injected plasma armature", Rev. Sci. Instrum. **80**, 083506 (2009).
- [16] MESSER, S., et al., "Fast pressure probe measurements of a high-velocity plasma plume", Phys. Plasmas **16**, 064502 (2009).
- [17] GALKIN, S. A., GJET-2D compressible gas dynamics, in-house code under development.
- [18] BOGATU, I. N., US patent pending.